

Self-organization of ascending-bubble ensembles

E. V. Barmina, N. A. Kirichenko, P. G. Kuzmin, and G. A. Shafeev

Wave Research Center of A.M. Prokhorov General Physics Institute of the Russian Academy of Sciences, 38 Vavilov Street,
119991 Moscow, Russian Federation

(Received 5 October 2012; revised manuscript received 7 February 2013; published 1 May 2013)

Self-organization of hydrogen bubbles generated by laser-treated areas of an aluminum plate etched in a basic aqueous solution of ammonia is studied experimentally and theoretically. The dynamics of the establishment of a stationary pattern of gas bubbles is experimentally shown. In the theoretical model, the velocity field of liquid flows around an ensemble of several bubbles is obtained. Modeling of the process of self-organization of gas bubbles is performed on the basis of a continuum model of a bubble jet. Under certain assumptions, the pressure of a diluted system of bubbles is described by an equation similar to that for nonideal gas, which follows the van der Waals equation of state. The model predicts an alignment of gas bubbles along bisectors of the laser-treated area limited by a square, which is in good agreement with experimental observations. Further development of the model leads to an equation with a negative diffusion coefficient that may be responsible for symmetry breakdown and pattern formation.

DOI: [10.1103/PhysRevE.87.053001](https://doi.org/10.1103/PhysRevE.87.053001)

PACS number(s): 47.20.Bp, 47.55.D-, 47.61.Jd

I. INTRODUCTION

A formation of dissipative structures is typical for open nonlinear systems [1]. Liquid flows in the field of gravity are characterized by a number of instabilities, e.g., Rayleigh–Bénard or Bénard–Marangoni convection. In some cases, these instabilities lead to a formation of self-organized structures, like the well-known Bénard cells that appear due to buoyancy force. The self-organized structures arise as the result of the amplification of microscopic fluctuations to the macroscopic level through bifurcation. The addition of small solid particles into the liquid is largely used for visualization of hydrodynamic flows. For example, fine aluminum powder (flakes) can be used to visualize either Bénard cells or Marangoni convection flows [2]. Sufficiently small solid particles that do not interact with one another are believed to be tracers of liquid flows. However, the suspended particles form their own trajectories under conditions of the Marangoni convection [2,3]. The particles are ordered into a symmetric closed trajectory that rotates with a certain angular velocity. The explanation for this has been suggested in a recent paper [4]. The deviation of particle trajectories from the hydrodynamic flow is due to their inertia. The resulting trajectory is the interplay between viscous drag forces and inertial behavior of the particle motion.

Another example of a two-phase system is a fluid with gas bubbles. Flows with a large bubble concentration occur in many natural and industrial processes, e.g., propeller-induced cavitation in ship building, cavitation in fluid machinery, nucleate boiling in reactors and similar devices, and many processes (centrifuges and mixers) in the chemical process industry. *A priori*, gas bubbles can hardly be considered tracers of hydrodynamic flows. In the gravity field, their motion is dominated by buoyancy force, which is compensated by a viscous Stokes force at the bubble–liquid interface. Big (0.1–0.2 cm in diameter) individual bubbles demonstrate the instability of their shape upon rising in water. Moreover, individual small bubbles rise rectilinearly, while larger bubbles follow a zigzag trajectory [5]. Rising bubbles can interact with one another. When a pair of bubbles rises in a still liquid

due to buoyancy, the bubbles are attracted toward each other when the angle between their line of centers and the vertical direction are in the range $[\theta_c, 180 - \theta_c]$ and repelled from each other when the angle and the vertical direction are outside the same range, θ_c being a critical angle ranging from 35° when the two bubbles are in contact to 54° when they are widely separated [6]. The adjacent bubbles interact with each other through the vorticity fields about them. Switching of bubble behavior occurs at some critical Reynolds number. Sufficiently close bubbles form a horizontal cluster that rises vertically, with their line of centers perpendicular to the rise in velocity [7]. Large (4–5 mm) bubbles tend to form a vertical cluster [8]. The type of clustering depends on the deformability of bubbles. According to the Bernoulli equation, higher fluid velocity in the wake of a bubble results in lower pressure, and the second bubble is shifted underneath. Rising of gas bubbles at a high concentration (20% and more) in the fluid is a collective effect and may induce the fluid flow due to viscous interaction. In turn, the liquid flow affects the motion of bubbles, so there is feedback between the flows of the liquid and the concentration of gas bubbles. This positive feedback may lead to the formation of dissipative structures made of gas bubbles.

Recently, we reported the process of self-organization of gas bubbles rising over a laser-etched surface of an aluminum target in a weakly basic aqueous solution [9]. Ascending bubbles formed various stationary structures, whose symmetry was determined by the symmetry of the etched area. Bubbles aligned along the bisectors of the contour of the etched area. For example, in case of a square-shaped laser-processed area, the bubbles aligned along diagonals of the square. The dynamics of the establishment of the stationary pattern of gas bubbles is presented in the sequence of frames in Fig. 1.

Bubbles became visible due to the scattering of light on them. The stationary distribution of gas bubbles was established ~ 5 min after dipping the laser-processed aluminum plate into an aqueous solution of ammonia (10%). The alignment of hydrogen bubbles along diagonals (attraction to diagonals) of the square laser-processed area was clearly seen.

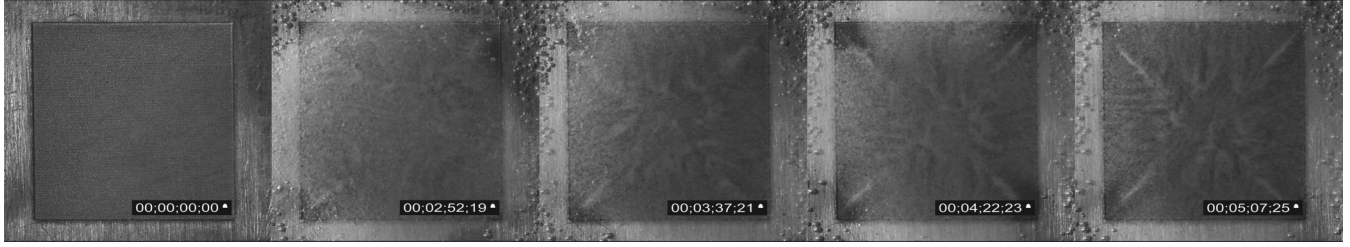


FIG. 1. Establishment of a stationary pattern of gas bubbles over a square laser-processed area of aluminum plate. Each frame shows the time elapsed from dipping the plate into the ammonia solution. The lateral dimensions of the square are 2×2 cm, and the thickness of the liquid layer is 5 mm.

The pattern remained until the depletion of the solution, which lasted up to several hours. Similar alignment was observed for other shapes of the laser-treated areas, e.g., triangles [9]. It is evident that individual bubbles interacted with one another through viscous liquid flows. The aim of this paper is to suggest a theoretical model of the self-organization of rising bubbles originating from the heaving of bubbles.

II. THEORETICAL MODEL

Let us build a model describing a stationary flow of gas bubbles ascending in a liquid in the field of gravity. The following realistic assumptions simplify a consideration but do not change the results qualitatively:

(1) According to the experimental data, the bubbles remain spherical upon rising with an almost constant radius R . The typical radius of bubbles observed in our experiments is $R \sim 50 - 100 \mu\text{m}$. This radius is established due to the equilibrium of gas pressure inside the bubble and hydrostatic pressure of the liquid.

(2) The concentration of bubbles n is small: $nR^3 \ll 1$.

The typical rising velocity of bubbles in our experiments is $u \sim 0.5$ cm/s. For the kinematic viscosity of water $\nu = \eta/\rho \approx 10^{-2}$ cm²/s, this corresponds to Reynolds number $\text{Re} \sim 0.4$. This means that the friction force of bubbles in the water can be estimated by the following expression:

$$\mathbf{F} = \mu R \rho \nu \mathbf{u}. \quad (1)$$

This expression is valid for small gas bubbles with radii up to $\sim 100 \mu\text{m}$ [10]. The coefficient μ depends on the properties of the liquid and varies in the region $4\pi < \mu < 6\pi$, depending on the quantity of a surface-active substance solved in the liquid. In our experiments surfactants were not used, which allows one to let $\mu = 6\pi$, as in the Stokes formula.

An equation of motion of a single gas bubble in a still liquid has the following form (see, e.g., [Ref. [10]]):

$$V_0 \left(\rho_g + \frac{1}{2} \rho \right) \frac{d\mathbf{u}}{dt} = -V_0 \nabla P + V_0 (\rho - \rho_g) \mathbf{g} - 6\pi R \eta \mathbf{u}, \quad (2)$$

where $V_0 = 4\pi R^3/3$ is the bubble volume, ρ is density of the liquid, and ρ_g stands for the gas density inside the bubble. Here, the symbol P stands for an addition to pressure in the liquid, which is created by moving bubbles, whereas the hydrostatic pressure is taken into account by the Archimedes force $V_0(\rho - \rho_g)\mathbf{g}$, included separately in Eq. (2).

The term $(\rho/2)$ in the brackets on the left-hand side of Eq. (2) takes added mass into account. Since the gas density within the bubble is small ($\rho_g \ll \rho$), one can rewrite Eq. (2) as follows:

$$\frac{d\mathbf{u}}{dt} = -\frac{2}{\rho} \nabla P - 2\gamma(\mathbf{u} - \mathbf{u}_0). \quad (3)$$

Here,

$$\mathbf{u}_0 = -\mathbf{g}/\gamma, \quad \gamma = 6\pi R \eta / \rho V_0 = 9\nu/2R^2. \quad (4)$$

Vector \mathbf{u}_0 is antiparallel to the gravity vector \mathbf{g} and represents the stationary velocity of a bubble rising in a still liquid when the buoyancy force and the Stokes force become equal. The typical measured value of rising is near $u_0 \sim 0.5$ cm/s. According to Eq. (4), this value corresponds to $R \approx 50 \mu\text{m}$.

The parameter γ determines the rate of the establishment of stationary rising and in our conditions is $\gamma \sim 10^3$ s⁻¹. A distance traveled by a bubble during the time γ^{-1} is $l \sim u_0/\gamma \sim 10^{-3}$ cm, which is small compared with the characteristic dimensions of a bubble stream in the present experiments. Therefore, with sufficient accuracy, one may let

$$\mathbf{u} = \mathbf{u}_0 - \frac{1}{\gamma\rho} \nabla P. \quad (5)$$

This means that the bubble acquires its velocity \mathbf{u} just after detachment from the aluminum plate.

If the liquid moves with an average local velocity \mathbf{v} , then the motion of the bubble should be considered relative to the liquid, $\mathbf{u} \rightarrow \mathbf{u} - \mathbf{v}$, and Eq. (5) takes the form

$$\mathbf{u} = \mathbf{u}_0 + \mathbf{v} - \frac{1}{\gamma\rho} \nabla P. \quad (6)$$

Since distances between bubbles are large, only the liquid flow caused by the bubble a large distance away is of interest. At distances $l \gg R$, the liquid can be treated as ideal because the corresponding Reynolds number is large: $\text{Re} = ul/\nu \gg 1$. Under these conditions, a velocity field of the liquid around the bubble with the radius R is given by the following expression [11]:

$$\mathbf{v} = \frac{R^3}{2r^3} [3\mathbf{n}(\mathbf{u}\mathbf{n}) - \mathbf{u}], \quad (7)$$

where $\mathbf{n} = \mathbf{r}/r$ is a unit vector along the radius vector starting from the center of the bubble. This flow has the potential

$$\varphi = -\frac{R^3}{2r^2} \mathbf{u}\mathbf{n}, \quad \mathbf{v} = \text{grad}\varphi. \quad (8)$$

Within the accepted assumptions, a distribution of pressures in a still liquid around the bubble moving with velocity \mathbf{u} is given by the formula [11]

$$P = \rho \mathbf{u} \mathbf{v} - \rho v^2 / 2 \quad (9)$$

or, according to Eq. (7),

$$P = -\rho \frac{1}{2} \left(\frac{R}{r} \right)^6 [3(\mathbf{u} \mathbf{n})^2 + \mathbf{u}^2] + \rho \frac{R^3}{2r^3} [3(\mathbf{u} \mathbf{n})^2 - \mathbf{u}^2]. \quad (10)$$

The first term in Eq. (10) behaves like $(R/r)^3$, while the second one decreases with distance like $(R/r)^6$ and is negligible at distances $r \gg R$. This means that the second term is significant only up to distances $r \sim 2R$, and with sufficient accuracy, at bubble concentration $n \ll R^{-3}$, we can set

$$P = \rho \mathbf{u} \mathbf{v}. \quad (11)$$

Since the system (gas) of bubbles is diluted, its influence on the liquid is small. In particular, the motion of the liquid induced by bubbles remains slow on average: $v \ll u_0$.

Therefore, the problem is reduced to a determination of the liquid velocity and pressure fields \mathbf{v} and P produced by all bubbles. A motion of single bubbles can then be calculated using the equation of motion [Eq. (6)] in the self-consistent fields \mathbf{v} and P :

$$\frac{d\mathbf{r}}{dt} = \mathbf{u}_0 + \mathbf{v}(\mathbf{r}) - \frac{1}{\gamma \rho} \nabla P(\mathbf{r}). \quad (12)$$

Consider a diluted gas of rising bubbles with local concentration $n(\mathbf{r})$. The velocity field of the liquid is given by the following expression:

$$\begin{aligned} \varphi(\mathbf{r}) &= \sum_i \varphi_1(\mathbf{r} - \mathbf{r}_i) = -\frac{1}{2} R^3 \sum_i \frac{(\mathbf{r} - \mathbf{r}_i) \mathbf{u}_i}{|\mathbf{r} - \mathbf{r}_i|^3}, \\ \mathbf{v} &= \text{grad} \varphi, \end{aligned} \quad (13)$$

where $\varphi_1(\mathbf{r} - \mathbf{r}_1)$ stands for the velocity potential at the point \mathbf{r} induced by a single bubble located at the point \mathbf{r}_1 and is given by Eq. (8).

An additivity of the potential φ used in Eq. (13) follows from a linearity of the Laplace equation $\Delta \varphi = 0$, which describes a laminar motion of an incompressible liquid ($\text{div} \mathbf{v} = 0$, $\mathbf{v} = \nabla \varphi$).

A real field of velocities of liquid flow is rather complicated. Locally, it is similar to an electric field produced by a system of dipoles, as can be seen from Eqs. (7) and (8). However, an averaged field is much smoother and is mainly determined by the motion of the liquid at distances much larger than the diameter of a single bubble.

A transfer to the mean field approximation can be achieved within the framework of a continuum description. Within this approach, we let the number of bubbles in the elementary volume dV be $n(\mathbf{r})dV$. Then, after replacing the summing by integration in Eq. (13), we obtain the next expression for the potential of the mean velocity field:

$$\varphi = -\frac{R^3}{2} \int \frac{(\mathbf{r} - \mathbf{r}_1) \mathbf{j}(\mathbf{r}_1)}{|\mathbf{r} - \mathbf{r}_1|^3} dV_1, \quad (14)$$

where the vector $\mathbf{j}(\mathbf{r}_1) = n(\mathbf{r}_1) \mathbf{u}(\mathbf{r}_1)$ stands for the density flux of bubbles. The expression in Eq. (14) is similar to the

well-known expression for the potential of an electric field within a medium with the polarization vector $\mathbf{P} = -nR^3 \mathbf{u} / 2 = -(R^3/2) \mathbf{j}$. Such an electrodynamic analogy is well known in hydrodynamics (see, e.g., [Ref. [12]]) and allows us to apply the methods of electrostatics for solving some hydrodynamics problems.

For further calculations, we rewrite Eq. (14) as follows:

$$\varphi = \frac{R^3}{2} \text{div} \int \frac{\mathbf{j}(\mathbf{r}_1)}{|\mathbf{r} - \mathbf{r}_1|} dV_1 = \frac{R^3}{2} \int \frac{\text{div} \mathbf{j}(\mathbf{r} - \mathbf{r}_1)}{|\mathbf{r}_1|} dV_1. \quad (15)$$

With the known potential $\varphi(\mathbf{r})$ and respectively the velocity of the liquid $\mathbf{v} = \nabla \varphi$, the pressure field can be found from Eq. (11).

The equation of continuity

$$\frac{\partial n}{\partial t} + \text{div} \mathbf{j} = 0 \quad (16)$$

should be added to the above equations because bubbles neither generate nor disappear in the bulk of the liquid. We now consider a stationary flow, which means that $\partial n / \partial t = 0$. The bubbles are generated on the surface of the laser-treated aluminum and disappear on the upper surface of the liquid. The influence of these surfaces can be taken into account as sources and sinks in Eq. (17). In particular, for a flat layer of liquid of height h along the axis z , one may write the following:

$$\text{div} \mathbf{j} = nu_z \delta(z) - nu_z \delta(z - h). \quad (17)$$

We constructed a closed model, which includes Eqs. (11), (12), (14), (16), and (17). A solution of this system allows us to find self-consistent mean fields of liquid velocities and pressures produced by the whole system of rising bubbles.

Let us consider the bubble jet starting at $z = 0$ (aluminum plate) and finishing at $z = h$ (free surface of the liquid). We restrict ourselves to the lowest order approximation to the parameter $n_0 R^3 \ll 1$.

Substituting the expression

$$\begin{aligned} \text{div} \mathbf{j} &= n(x, y, 0) u_z(x, y, 0) \delta(z) \\ &\quad - n(x, y, h) u_z(x, y, 0) \delta(z - h) \end{aligned}$$

into Eq. (15), one obtains

$$\begin{aligned} \varphi &= \frac{1}{2} R^3 \left(\int \frac{u_0 n_0(x_1, y_1)}{\sqrt{(x - x_1)^2 + (y - y_1)^2 + z^2}} dx_1 dy_1 \right. \\ &\quad \left. - \int \frac{u_z(x_1, y_1, h) n(x_1, y_1, h)}{\sqrt{(x - x_1)^2 + (y - y_1)^2 + z^2}} dx_1 dy_1 \right), \end{aligned}$$

where $n_0(x, y) = n(x, y, 0)$ is an initial distribution of the bubble concentration. Using the condition $nR^3 \ll 1$, we may let $nu_z|_{z=h} \approx n_0 u_0$. This assumption is supported by the bubble flow being nearly symmetric relative to the middle ($z = h/2$) of the jet. As a result, we get an explicit expression for the velocity potential:

$$\begin{aligned} \varphi &= \frac{1}{2} R^3 u_0 [\psi(x, y, z) - \psi(x, y, h - z)], \quad \mathbf{v} = \nabla \varphi, \\ \psi(x, y, z) &= \int \frac{n_0(x_1, y_1) dx_1 dy_1}{\sqrt{(x - x_1)^2 + (y - y_1)^2 + z^2}}. \end{aligned} \quad (18)$$

First, we mention a special case in which the plate generating bubbles is a ring with the radius R_0 . The liquid layer thickness

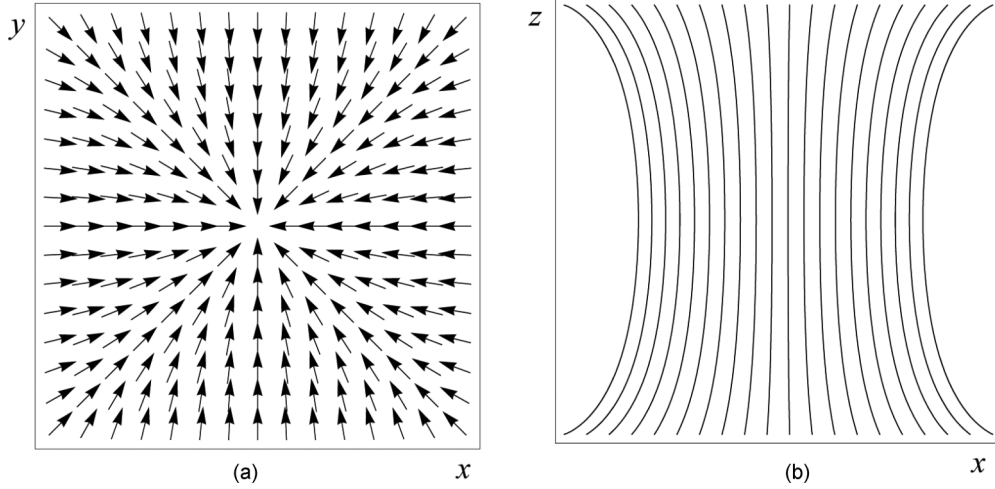


FIG. 2. Field of bubble velocities. (a) Top view. (b) Cross-section of the bubble jet at $y = a/2$. $n_0 R^3 = 0.2$, $h = a$.

is assumed to be large: $h \gg R$. Then, the liquid velocity field along the axis going through the center of the ring perpendicular to the plate is given by

$$v(z) = -\pi R^3 n_0 u_0 \left(1 - \frac{z}{\sqrt{R_0^2 + z^2}} \right).$$

Its derivative at $z = 0$ equals

$$\partial v / \partial z|_{z=0} = \pi R^3 n_0 u_0 / R_0, \tag{19}$$

which gives a maximum value of $\partial v / \partial z$. This estimation gives typical values of the velocity derivatives for different shapes of the plate with characteristic sizes of $\sim R_0$.

Note also the next similarity law. Let the plate generating bubbles be a square. Denote the liquid velocity field for a square with the size 1×1 a.u. as $\mathbf{v}_0(\mathbf{r})$. Then, the field $\mathbf{v}(\mathbf{r})$ produced by bubbles rising from the square plate with sizes

$a \times a$ is given by the formula $\mathbf{v}(\mathbf{r}) = \mathbf{v}_0(\mathbf{r}/a)$. This result directly follows from Eq. (18).

We now are able to investigate the motion of individual bubbles. Their trajectories can be found from Eq. (12). Using the estimation in Eq. (19), we can evaluate the ratio of the last term in Eq. (12) to u_0 :

$$\varepsilon = \frac{1}{\gamma \rho u_0} |\nabla P| = \frac{1}{\gamma u_0} |\nabla(\mathbf{u}\mathbf{v})| \approx \frac{1}{\gamma} \frac{\partial v}{\partial z} \sim \frac{1}{\gamma R_0} \pi R^3 n_0 u_0.$$

For the typical parameters of our experiments $\gamma \sim 10^3 \text{ s}^{-1}$, $R_0 \sim 1 \text{ cm}$, and $u_0 \sim 0.5 \text{ cm/s}$, we get $\varepsilon \sim 10^{-3} n_0 R^3 \ll 1$. This means that the last term in Eq. (12) is negligible and the equation of motion of a bubble is simplified as

$$\frac{d\mathbf{r}}{dt} = \mathbf{u}_0 + \mathbf{v}, \tag{20}$$

where the field $\mathbf{v}(\mathbf{r})$ should be calculated using Eq. (18).

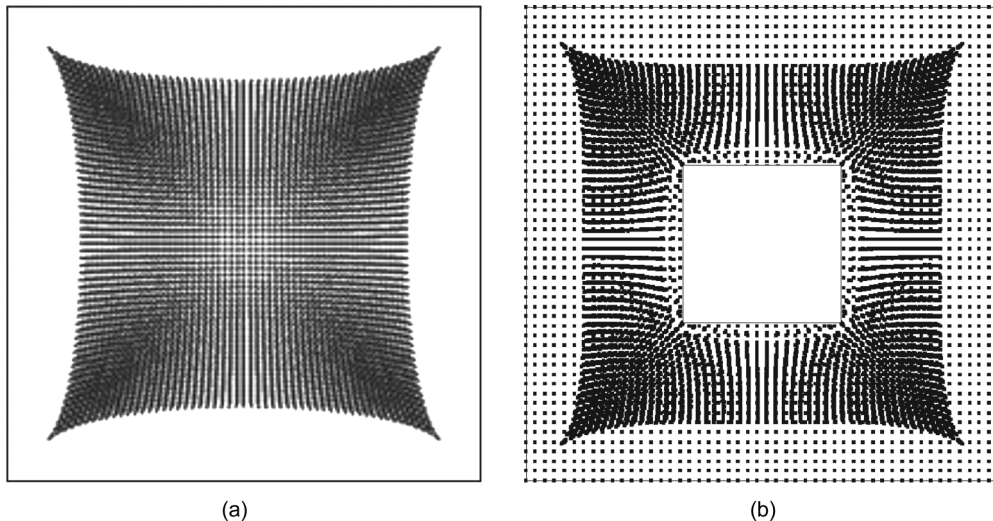


FIG. 3. (a) Top view of the bubble jet in the region $h < 4 < z < 3h < 4$. The density of the image is proportional to the optical density of the liquid layer with bubbles. The boundary square indicates the target, which generates bubbles. (b) The same as in Fig. 3(a) except that the central part of the target is inactive. The size of the inactive region is $1 < 3 \times 1 < 3$ a.u..

III. NUMERICAL RESULTS

The constructed model was numerically investigated. The coordinate origin is located in the geometric center of the target, so the target has coordinates

$$z = 0, \quad -a/2 \leq x \leq a/2, \quad -a/2 \leq y \leq a/2.$$

Figure 2 shows a calculated vector field of bubble velocities when the etched area of the target has the square shape $a \times a$, within which $n_0(x, y) = \text{const}$ while outside the square $n_0(x, y) = 0$. The thickness of the liquid layer h was taken as $h = a$. Figure 2(a) presents the vector field of bubble velocities at the section $z = 0.1a$ of the jet. Figure 2(b) illustrates the trajectories of bubbles in the vertical cross-section of the jet at $y = a/2$, a numerical solution of Eq. (20) together with Eq. (19). Figure 2(a) clearly demonstrates the effect of the retraction of bubbles into motion along the diagonals of the square, similar to that observed in the experiment. Moreover, the jet shrinks with height because of the entrainment effect [Fig. 2(b)], like that reported in previous experiments [9].

To illustrate observable changes in bubble concentration, consider the region of the jet around the middle part: $h/4 < z < 3h/4$, where the compression of the jet reaches maximum. The optical thickness of this region

$$N(x, y) = \int_{h/4}^{3h/4} n(x, y, z) dz \quad (21)$$

is presented in Fig. 3(a). In the calculations, a grid with the steps $\Delta x = \Delta y = a/55$, $\Delta z = h/10$ was used, and a point plot was built up. The alignment of bubbles along the diagonals of the square is clearly observed, similar to experimental observations.

Similarly, we calculated the point plot for different target plate shapes. As an example, Fig. 3(b) shows the top view when the central part of the plate is inactive; i.e., it does not generate bubbles. A similar picture was observed in experiments.

IV. FURTHER DEVELOPMENT OF THE MODEL

In the above consideration, the concentration of bubbles was assumed to be small so that the term $-\rho v^2/2$ in pressure [see Eq. (9)] could be ignored. However, as has been demonstrated, the concentration of bubbles increases because of the entrainment effect and reaches its maximum in the axial region [Fig. 2(b)]. In addition, in the middle part of the jet, the role of the boundary surfaces of the liquid decreases but the flow velocity remains finite. Therefore, the term $(-\rho v^2/2)$ may become essential. This term also has a special role because it depends slightly on the distance from borders of the liquid and is determined by the local value of bubble velocities, thus affecting their motion along the whole jet. Let us consider the influence of this term in more details.

The corresponding contribution to pressure induced by a single bubble is given according to Eqs. (8) and (9) by the following expression:

$$P_b = -\rho \frac{1}{2} \left(\frac{R}{r} \right)^6 [3(\mathbf{u}\mathbf{u})^2 + \mathbf{u}^2] \quad (22)$$

where the index b indicates the bulk effect. For a noncoherent system of bubbles, the pressure equals

$$P_b = -\rho \frac{R^6}{2} \sum_i \frac{3(\mathbf{u}(\mathbf{r}_i)(\mathbf{r} - \mathbf{r}_i))^2 + \mathbf{u}^2(\mathbf{r}_i)|\mathbf{r} - \mathbf{r}_i|^2}{|\mathbf{r} - \mathbf{r}_i|^8} n(\mathbf{r}_i). \quad (23)$$

A direct transition from summing to integration in this case is impossible, since the corresponding integral diverges in the vicinity of the bubble ($\sim \int_r^\infty r^{-6} \cdot r^2 dr \sim r^{-3}$); thus, an alternative approach should be applied.

Let us again assume that the ‘‘bubble gas’’ is diluted: $nR^3 \ll 1$. The pressure in Eq. (22) decreases rapidly with distance from the bubble, so the pressure near a single bubble is induced only by its nearest neighbors. For example, if bubbles are arranged into a simple cubic lattice, then there exist only 26 neighbor bubbles, which should be taken into account. This means that $P = CP_1$, where $C \sim 10$ and P_1 stands for an averaged pressure induced by one nearest bubble. According to Eq. (22), a contribution of all other bubbles is at least 2^6 times smaller. If a mean distance between the two nearest bubbles is d , then the concentration of bubbles is $n = 1/d^3$. In reality, the bubbles are arranged chaotically, so we can write the dependence of the pressure P on the bubble concentration n as follows:

$$P_b = -\frac{1}{2} C \rho R^6 n^2 [3(\overline{\mathbf{u}\mathbf{u}})^2 + \overline{\mathbf{u}^2}] \approx -C_0 \rho R^6 n^2 u^2, \quad (24)$$

where $C_0 \sim C \sim 10$ is a numerical coefficient and averaging is performed over all directions.

The expression P_b is quite similar to the pressure of nonideal gas, which follows the van der Waals equation.

Far from the borders of the liquid layer, liquid flow is negligible, which follows directly from Eq. (18), and pressure is determined only by the term in Eq. (24). Then, according to Eq. (6), the bubble velocity is described by the expression

$$\mathbf{u} = \mathbf{u}_0 + \frac{C_0 R^6}{\gamma} \nabla(n^2 u^2). \quad (25)$$

The nonstationary equation of continuity

$$\frac{\partial n}{\partial t} + \text{div}(n\mathbf{u}) = 0$$

takes on the form

$$\frac{\partial n}{\partial t} + u_0 \frac{\partial n}{\partial z} + D \text{div}(n^2 \nabla n) = 0, \quad D = \frac{2}{\gamma} C_0 R^6 u_0^2. \quad (26)$$

This is a diffusion equation with a negative diffusion coefficient that depends on the concentration ($-Dn^2$). Because of the properties of such equations, they can describe certain types of instabilities. In particular, there may arise a self-compression effect [13].

To outline an appearance of this effect, let us consider a spatially uniform flow of bubbles with $n(\mathbf{r}) = n_0 = \text{const}$, $\mathbf{u} = \mathbf{u}_0 = \text{const}$. If a perturbation of homogeneity arises, it should evolve according to Eq. (26). Consider the time-independent one-dimensional case. Let

$$n(x, y, z) = n_0 + n_1(x, z), \quad |n_1| \ll n_0.$$

To simplify, we confine ourselves to perturbations evolving in two dimensions: x and z . Linearization of Eq. (26) gives

$$\frac{\partial n_1}{\partial z} + \mu \left(\frac{\partial^2 n_1}{\partial x^2} + \frac{\partial^2 n_1}{\partial z^2} \right) = 0, \quad \mu = \frac{Dn_0^2}{u_0}. \quad (27)$$

Let us look for a solution of the Cauchy problem for this equation in the form

$$n_1(x, z) = n_{10} \exp(iq_x x + iq_z z). \quad (28)$$

Substituting this expression into Eq. (27) gives the dispersion equation

$$\mu(q_x^2 + q_z^2) - iq_z = 0,$$

which defines the two branches of spectrum:

$$q_z^{(1)} = \frac{i}{2\mu}(1+p), \quad q_z^{(2)} = \frac{i}{2\mu}(1-p), \quad (29)$$

$$p = \sqrt{1 + 4\mu^2 q_x^2} > 1.$$

It is essential that $\text{Im}q_z^{(2)} < 0$, which indicates instability of the solution of the Cauchy problem. Assuming the parameter μ to be small enough ($\mu \ll \delta_0$), we may use an approximate expression $p \approx 1 + 2\mu^2 q_x^2$. Let us take an initial perturbation of the form

$$n_1(x, 0) = n_{10} \exp(-x^2/\delta_0^2). \quad (30)$$

Then, using the spectrum in Eq. (29) and applying standard techniques, we can obtain

$$n_1(x, z) = \int_{-\infty}^{\infty} \frac{dq_x}{2\pi} \int_{-\infty}^{\infty} n_0(x_1) \exp[iq_x(x-x_1) + iq_z z] dx_1$$

$$= \sim n_{10} \frac{\delta_0}{\delta(z)} \exp\left(-\frac{x^2}{\delta^2(z)}\right), \quad (31)$$

where the effective width of the perturbation is $\delta(z) = \sqrt{\delta_0^2 - 4\mu z}$.

We retained in Eq. (31) the main term, which describes an increasing amplitude of perturbation

$$n_1(0, z) \sim \frac{n_{10}}{\sqrt{1 - 4\mu z/\delta_0^2}} \quad (32)$$

with a simultaneous shrinking of the width $\delta(z)$ —the so-called effect of sharpening with localization, which is characteristic for nonlinear media of different kinds [13]. This mechanism increases the contrast of the structures discussed above but may also lead to the creation of other types of structures.

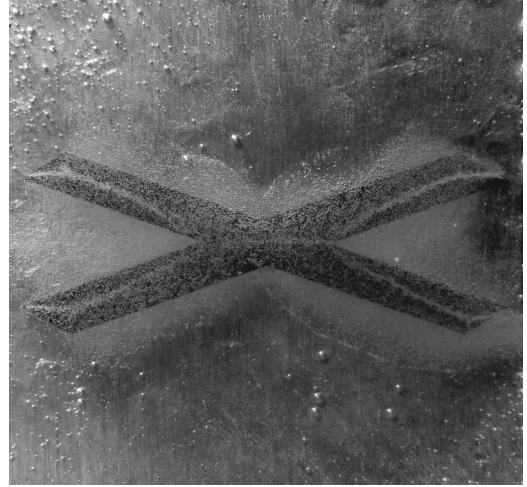


FIG. 4. Stationary pattern of gas bubbles over an X-shaped area of aluminum plate. The lateral size of the plate is 3×3 cm.

An example of such instability is presented in Fig. 4. Here, the aluminum plate was exposed to laser radiation in such a way that the etched area was X shaped. Then the plate was dipped into a basic solution. The stationary distribution of bubbles is achieved after a certain time of etching. One can see that bubbles are arranged along the bisectors at the ends of X-shaped area. In the middle, they are situated in the middle of the etched area, though as the distance between two adjacent jets of bubbles reaches some critical value, the jets start an interaction. Finally, in the middle of the X-shaped area, they are united. Figure 4 illustrates that individual jets of bubbles can interact with one another. In some experimental conditions, this may lead to the symmetry breakdown that is described by Eq. (26). These studies are ongoing.

V. CONCLUSION

A model of self-organization of gas bubbles over a spatially confined etched area has been developed. This model shows good agreement with experimentally observed stationary patterns of gas bubbles over confined areas of etching. It also shows that under certain assumptions, the pressure of diluted gas bubbles is described by an equation similar to that for nonideal gas, which follows the van der Waals equation of state. Further development of the model results in an equation with a negative diffusion coefficient, which depends on the concentration of bubbles. The derived model predicts the formation of other types of structures made of ascending gas bubbles.

- [1] I. Prigogine, *Introduction to Thermodynamics of Irreversible Processes*, 2nd ed. (John Wiley and Sons, New York, 1961).
- [2] D. Schwabe, A. I. Mizev, M. Udayasankar, and S. Tanaka, *Phys. Fluids* **19**, 072102 (2007).

- [3] D. Schwabe, P. Hintz, and S. Frank, *Microgravity Sci. Technol.* **9**, 163 (1996).
- [4] D. O. Pushkin, D. E. Melnikov, and V. M. Shevtsova, *Phys. Rev. Lett.* **106**, 234501 (2011).
- [5] M. Wu and M. Gharib, *Phys. Fluids* **14**, L49 (2002).

- [6] D. Legendre, J. Magnaudet, and G. Mougin, *J. Fluid Mech.* **497**, 133 (2003).
- [7] L. van Wijngaarden, *J. Fluid Mech.* **251**, 55 (1993).
- [8] J. Martinez Mercado, D. Chehata Gomez, D. van Gils, C. Sun, and D. Lohse, *J. Fluid Mech.* **650**, 287 (2010).
- [9] E. V. Barmina, P. G. Kuzmin, and G. A. Shafeev, *Phys. Rev. E* **84**, 045302(R) (2011).
- [10] A. G. Petrov, *Analytical Hydrodynamics* (Fizmatlit, Moscow, 2010) (in Russian).
- [11] L. D. Landau and E. M. Lifshitz, *Course of Theoretical Physics*, 2nd ed. (Butterworth-Heinemann, Oxford, UK, 1987), Vol. 6.
- [12] L. G. Lojtsjanskij, *Mechanics of Liquid and Gas* (Nauka, Moscow, 1973) (in Russian).
- [13] A. A. Samarskii, V. A. Galaktionov, S. P. Kurdjumov, and A. P. Mikhailov, *Regimes with Sharpening in the Problems for Quasilinear Parabolic Equations* (Nauka, Moscow, 1987) (in Russian).